Journal of Tissue Viability 35 (2026) 100977

Contents lists available at ScienceDirect

Journal of Tissue Viability

journal homepage: www.elsevier.com/locate/jtv

# Be there or be square: Should we adopt non-rectangular dressing shapes in single-use negative pressure wound therapy?

Ofek Barzilay [a], Amit Gefen [a,b,c,*]

[a] School of Biomedical Engineering, Faculty of Engineering, Tel Aviv University, Tel Aviv, Israel
[b] Ghent University, Skin Integrity Research Group (SKINT), University Centre for Nursing and Midwifery, Department of Public Health and Primary Care, Ghent, Belgium
[c] Department of Mathematics and Statistics and the Data Science Institute, Faculty of Sciences, Hasselt University, Hasselt, Belgium

ARTICLE INFO

*Keywords:*
Dressing design and shape optimization
Wound healing biomechanics
Computational finite element modeling and simulations
Mechanobiology in wound care
Skin and subdermal tissue stress concentrations

ABSTRACT

*Background:* Single-use negative-pressure wound therapy (suNPWT) dressings for closed surgical incisions are predominantly rectangular, despite long-time evidence from biomechanics that sharp or small-radius corners generate localized stress concentrations in underlying tissues. Optimizing dressing geometry and stiffness distribution may reduce the peri-incisional stress concentrations and improve closure.

*Objectives:* To determine how dressing shape and regional stiffness variations influence the peri-wound skin stresses and stress concentrations and the incision closure biomechanics under a negative pressure level of −125 mmHg.

*Methods:* A validated three-dimensional finite element model of a sutured midline incision was developed. Five homogeneous dressing shapes (rectangular, circular, elliptical, stadium, and dome) of identical contact area and material properties were compared for reduction in peak lateral skin stresses (ΔS). The best-performing dressing shape underwent further testing in eight stiffness configurations (homogeneous, or with stiffer/softer peripheral regions in symmetric or axisymmetric patterns). The lateral displacement of the peri-wound skin was used as a measure for the closure work. A sensitivity analysis was conducted on chosen model variants for broader transferability and for exploring potential covariance between dressing shape and material properties.

*Results:* Among the homogeneous dressing shapes, the circular dressing achieved the greatest stress reduction (ΔS = 2.9 %) versus the rectangular control (0.9 %). In the circular form, incorporating a stiffer peripheral symmetric ring around a softer core improved performance (ΔS = 3.2 %) while maintaining substantial lateral displacement (3.35 mm), achieving an optimal combination of stress relief with closure assistance. A fully stiff homogeneous dressing maximized the ΔS (6.5 %) but provided negligible closure support, whereas a fully soft dressing behaved conversely. The sensitivity analysis did not change these quantitative rankings across the studied model variants.

*Conclusions:* Eliminating sharp or small-radius geometric discontinuities and tuning the regional stiffness can markedly attenuate peri-incisional stresses without compromising the contribution of the dressing to the closure work. Circular suNPWT dressings with a peripheral stiffer ring offer a biomechanically superior, manufacturable alternative to conventional rectangular designs, warranting further pre-clinical and clinical evaluations.

## 1. Introduction

Negative pressure wound therapy (NPWT) is widely used to treat complex acute and chronic wounds by applying subatmospheric pressure through a foam dressing connected to a suction pump system [1,2]. When applied to closed surgical incisions, NPWT has been shown to improve healing by enhancing perfusion, reducing edema, seroma, and hematoma formation, and minimizing lateral mechanical stresses by drawing the wound edges together [2–4]. However, the mechanical process of the primary closure itself, using sutures, staples or even the more modern zippers, introduces stress concentration exposures to the skin and underlying tissues, potentially resulting in tissue necrosis, incision dehiscence, abnormal scarring and increased risk of surgical site infections [5–7]. Single-use NPWT (suNPWT) systems have been shown to mitigate these tissue stress concentrations near closed incisions,

* Corresponding author. Biomedical Engineering, The Herbert J. Berman Chair in Vascular Bioengineering, School of Biomedical Engineering, Faculty of Engineering, Tel Aviv University, Tel Aviv, 69978, Israel.
*E-mail address:* gefen@tauex.tau.ac.il (A. Gefen).

https://doi.org/10.1016/j.jtv.2025.100977
Received 9 August 2025; Received in revised form 27 October 2025; Accepted 1 December 2025
Available online 4 December 2025

**Abbreviations**

| | |
|---|---|
| AB | Adhesive base |
| FE | Finite element |
| NPWT | Negative pressure wound therapy |
| PU | Polyurethane |
| suNPWT | Single-use negative pressure wound therapy |

supporting the hypothesis that post-closure application of suNPWT can play an active biomechanical role in wound healing [4]. Despite this, the design of commercial suNPWT systems remains largely conventional. In particular, rectangular foam dressings dominate the market, driven by clinical habits and the design choices of leading manufacturers [8–10]. This design choice appears to persist despite longstanding knowledge in mechanical engineering that geometric discontinuities such as edges and corners, which are in this case, the corners of the dressing, create stress concentrations in the underlying soft tissues, particularly the skin [11, 12]. For example, corners on buildings are known to cause wind turbulences, and likewise dressing corners may disrupt the tissue stress flow. Furthermore, under the negative pressure generated by suNPWT, any mismatch between the stiffness of the applied dressing and the surrounding skin, combined with the sharp corners of rectangular dressings, leads to localized stress concentrations rather than a uniform redistribution of the mechanical loads [11,12]. While polyurethane (PU) foam remains the industry standard for the absorptive layer in NPWT dressings, due to the porosity, flexibility, and pressure transmission characteristics, its uniform and isotropic properties may limit the potential biomechanical contribution of the dressing to wound healing [13, 14].

In the above context, it is surprising that a major gap still exists in the literature with regards to the contribution of the suNPWT dressing shape or internal stiffness distribution to the mechanical loading state which effectively promotes incision closure. Namely, information is missing regarding the contribution of the dressing shape and stiffness distribution factors to reducing the tissue stress concentrations around the primary closure sites, e.g., the puncture points of sutures or staples, or the attachment sites of adhesive bases for zippers. Prior computational modeling work has used finite element (FE) analysis to investigate the biomechanical effects of NPWT, examining variables such as dressing material (foam versus gauze), pressure levels, and tissue stiffness level [13–15]. However, these studies often relied on simplified 2D cross-sectional models, missing important out-of-plane effects. Our previous 3D FE work has shown that non-invasive closure techniques reduce peri-incisional stresses compared to sutures [5], that increasing the uniform stiffness of dressings does not significantly alter the skin stress distributions [16], and that suNPWT following closure effectively contributes to the lateral closure work and reduces peri-wound mechanical stress concentrations [4].

The current study builds on these foundations by systematically exploring, using FE modeling and simulations, whether two under-investigated parameters: the dressing shape and internal stiffness distribution, can be purposefully optimized to further reduce peri-incisional stress concentrations and improve the mechanical support of incision closure. Our goal was to identify an optimal suNPWT dressing configuration that balances these two parameters, thus offering a potentially superior dressing design for suNPWT systems applied to surgical incisions.

## 2. Methods

### 2.1. The model variants and their geometry

All the model variants, testing different suNPWT foam dressing designs (shapes and material compositions), included an elliptical surgical incision with skin surface-plane dimensions of 75 × 8 mm (length × width) (Fig. 1a). This incision extended through skin, adipose and skeletal muscle tissues (Fig. 1a). The thicknesses of the skin, adipose and muscle were maintained at 2, 18 and 9 mm, respectively, across all the model variants (Fig. 1a). Primary closure was modelled using adhesive zippers replicating a typical geometry and configuration of a commercial closure device (Fig. 1a). The adhesive zippers were modelled as four identical pairs of adhesive bases (ABs), with each pair consisting of two matching ABs mirrored with respect to the YZ plane (Fig. 1a). Each base was a thin trapezoidal shell with dimensions of 16 × 20 × 30 mm (short base x long base x height), positioned 10 mm apart (Fig. 1a). Each pair of ABs contained four zippers, spaced 4 mm apart.

The primary closure of the modelled incision was followed by application of a suNPWT system incorporating a foam dressing. Each model variant included a differently shaped suNPWT dressing, and material compositions of the dressings varied as well. With respect to shape, dressings were modelled as foam layers having different shapes and dimensions, however, their contact surface area with skin was always 100 $cm^2$ and their maximum thickness was set as 1.85 cm. The specific different dressing shapes were rectangular, circular, elliptical, stadium-shaped (a rectangle with semicircular ends), and dome-shaped (a section of a sphere). The dressing in each model variant was initially positioned 0.5 mm above the incision (to simulate the clinical application process), so that the longest aspect of the wound pad was aligned with the widest dimension of the incision, ensuring that the dressing fully covered the incision post application, as would have been performed clinically (Fig. 1b). The overall model dimensions (i.e. the geometrical model domain) were 375 × 400 × 29 mm (length × width × height), leaving sufficient margins around the surgical site and applied dressing to minimize potential boundary effects in accordance with Saint-Venant's principle (Fig. 1).

### 2.2. Mechanical properties of model components

All the model components were assumed to behave as hyperelastic Neo-Hookean materials, with a strain energy density function:

$$\boldsymbol{W} = \boldsymbol{C_{10}}(\overline{\boldsymbol{I_1}} - \boldsymbol{3}) + \frac{\boldsymbol{1}}{\boldsymbol{D_1}}(\boldsymbol{J} - \boldsymbol{1})^{\boldsymbol{2}} \quad (1)$$

where $C_{10}$ and $D_1$ are material-specific parameters related to shear resistance and compressibility, respectively, $\overline{I_1}$ is the first invariant of the right Cauchy-Green deformation tensor, and $J$ is the determinant of the deformation gradient tensor. The values of $C_{10}$ and $D_1$ for all the tissues and the ABs were selected based on the literature and applied to the different shapes of dressings (Table 1). After identifying the superior dressing shape, in terms of reduction of the skin stress concentrations associated with the primary closure (see Results section, Table 2), regional variations in mechanical properties of dressings were further introduced to explore whether additional improvement in the stress state of skin is possible, and whether these regional variations in dressing stiffness can also assist the incision-closure process under suNPWT. The specific mechanical properties assigned to each region of the dressings are listed in Table 3.

### 2.3. Interface and loading conditions

The side faces of the model were fixed for all translations and rotations, to consider the continuum interactions of the incorporated soft tissue with tissues outside the geometrical model domain, whereas the superior (skin side) and inferior surfaces of the model were allowed to move in response to the applied negative pressures. The contacts between the different tissue layers (skin-adipose and adipose-muscle) were all set as 'tie' ('no-slip condition') (Fig. 1a). Likewise, a 'tie' contact was defined between the ABs and the skin. The function of the zippers to

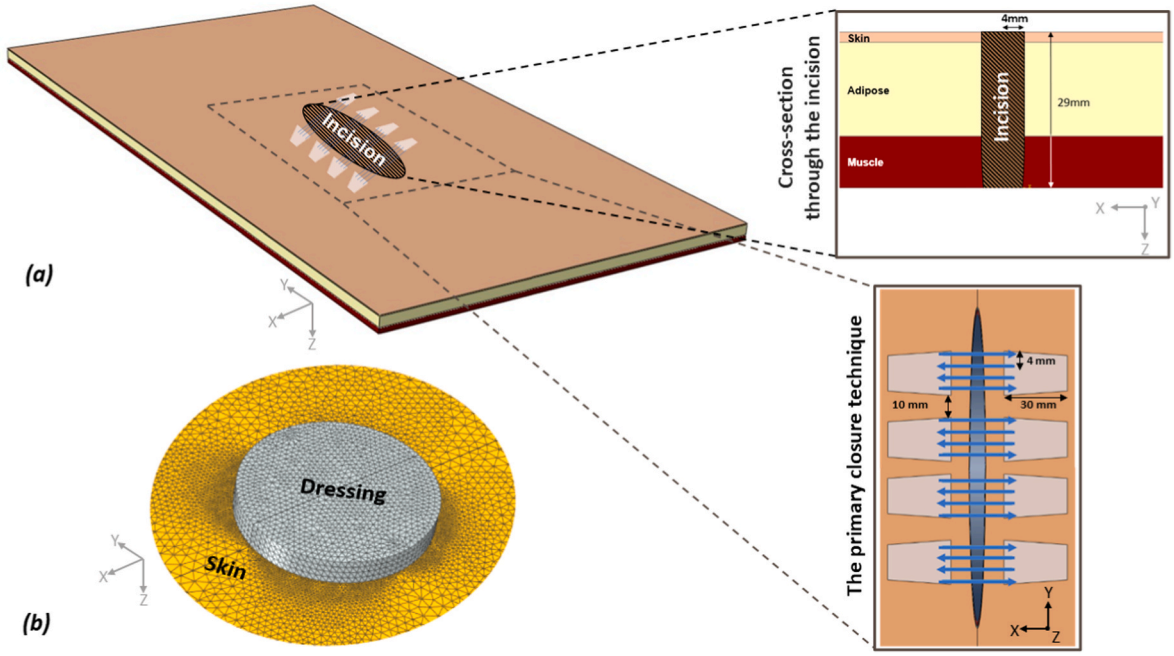


**Fig. 1.** The geometry (a) and finite element mesh (b) of the incision model. Details on the geometrical features and dimensions of the cross-section of the incision model, and on the primary closure technique using adhesive zippers, are provided in the top and bottom right frames, respectively. The mesh of the peri-wound model is shown here with a circular (negative pressure) uniform foam dressing placed over the incision in this particular example (note the increased mesh density nearer the dressing borders to achieve precision in calculations).

**Table 1**
Mechanical properties of the model components and variant dressing shapes.

| Model component | Coefficients | | Number of elements[e] |
|---|---|---|---|
| | $C_{10}$ [MPa] | $D_1$ [MPa$^{-1}$] | |
| Skin | 17.225[a] | ~0.0024[a] | 31,858–32,558 |
| Adipose | 0.0017[a] | 23.54[a] | 103,832–107,279 |
| Muscle | 2.875x10$^{-4}$[b] | 3.03[a] | 71,552–75,082 |
| Adhesive zippers | 193[c] | 0.0008[c] | 960 |
| Foam dressing | 0.00288[d] | 160[d] | 11,518–23,331 |

[a] Katzengold et al., 2018 [20].
[b] Palevski et al., 2006 [21].
[c] INEOS Olefins & Polymers USA. A60-70-162 Polyethylene Homopolymer: Technical Data Sheet. 2014 [22].
[d] Orlov & Gefen, 2022 [4].
[e] The variation in the number of elements results from the use of different dressing shapes, which. require different numbers of elements in the model components to achieve optimal element alignment.

generate the closure forces on the incision was simulated by displacing two of the nodes in each AB towards the incision, thus simulating the zipping action to fasten the peri-wound skin at the opposing sides of the incision (Fig. 1a). Subsequently, application of the suNPWT dressing by a clinician was simulated, by displacing the entire dressing towards the skin above the incision site (i.e., along the Z direction), until full dressing-skin contact was established (Fig. 1b). Once this contact was achieved, the suNPWT dressing was considered fully adhered to the peri-wound skin, meaning that no slippage was allowed between the dressing and skin in further simulation steps. Negative pressure was simulated as a uniform hydrostatic compression of −125 mmHg (representative of commercial suNPWT systems in the mainstream of the market of these devices). The negative pressure was simultaneously applied to all the six surfaces of the dressing (that is, the superior aspect, inferior aspect and the four lateral sides), resulting in a substantial reduction of the volumes of dressing (depending on the specific dressing shape and material properties).

### 2.4. Numerical method and computational resources

The FE modelling work including the geometrical setup, meshing, simulations, and all the analyses were conducted using Abaqus/CAE 2023 with its standard static solver, which is suitable for nonlinear, large-deformation problems. The meshing was performed semi-automatically, with manual refinements to increase the element density near the dressing-skin interface and around the edges of the incision (Fig. 1b). All the mesh elements were tetrahedral. The numbers of elements used for each tissue, AB and dressing component are listed in Tables 1 and 3 To reduce computational costs, and given that for all the

**Table 2**
Morphological indices of the variant dressing shapes.

| Index | Dressing shape | | | | |
|---|---|---|---|---|---|
| | 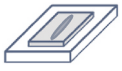 | 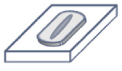 | 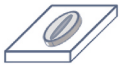 |  |  |
| Circularity[a] | 0.7 | 0.81 | 0.93 | 1 | 1 |
| Roundness[b] | 0.51 | 0.52 | 0.64 | 1 | 1 |
| R[a] | 0.84 | 0.98 | 0.99 | 0.99 | 0.99 |

[a] R = Circularity corrected by aspect ratio: Takashimizu et al., 2016 [23].
[b] Ritter et al., 2009 [24].

**Table 3**
Mechanical properties of the circular dressings with varying stiffness regions.

| Dressing | Region in dressing | Coefficients | | Number of elements |
|---|---|---|---|---|
| | | $C_{10}$ [MPa] | $D_1$ [$MPa^{-1}$] | |
| 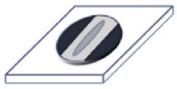 | Core- | 0.00288 | 160 | 9696 |
| | Stiffer wings | 0.02 | 30 | 4697 |
|  | Core | 0.00288 | 160 | 9696 |
| | Softer wings | 0.0015 | 200 | 4697 |
| 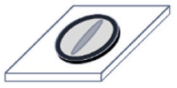 | Core | 0.00288 | 160 | 10648 |
| | Stiffer symmetric ring | 0.02 | 30 | 6858 |
|  | Core | 0.00288 | 160 | 10606 |
| | Softer symmetric ring | 0.0015 | 200 | 6858 |
| 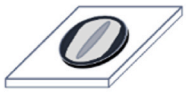 | Core | 0.00288 | 160 | 6298 |
| | Stiffer axisymmetric ring | 0.02 | 30 | 7530 |
|  | Core | 0.00288 | 160 | 6298 |
| | Softer axisymmetric ring | 0.0015 | 200 | 6647 |
| 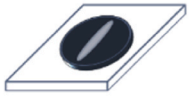 | Homogeneously stiff | 0.02 | 30 | 12970 |
|  | Homogeneously soft | 0.0015 | 200 | 12970 |

model variants, the computational problem is always axisymmetric around the incision line, only half of the geometry was constructed and numerically solved per model variant. Following the full convergence and completion of each simulation, the half-model was mirrored with respect to the XZ plane to reconstruct the full model and computational results for visualization purposes (Fig. 1). Each model variant required approximately 43 min to solve per simulation, on a 64-bit Windows 10 workstation equipped with an Intel® Core™ i7-9700X CPU (3.00 GHz) and 32 GB RAM.

### 2.5. Protocol of simulations and outcome measures

***'Shape' model variants***: First, five 'shape' model variants were simulated, each incorporating a different dressing shape, but all had identical foam mechanical properties (as noted in Table 1). Each such 'shape' model variant was analyzed to evaluate the maximum effective lateral stresses in skin around the AB-zipper attachment sites, where stress concentrations occurred (Fig. 2). These peak stresses were calculated both after the primary closure and prior to the simulated application of the suNPWT system, and following application of the suNPWT system, to isolate and quantify the contribution of the suNPWT system application to reduction of lateral skin stresses in the peri-wound. For each dressing shape (Fig. 3a), the lateral skin stress changes were calculated as:

$$\Delta S = \frac{S_{NP} - S_{PC}}{S_{PC}} \cdot 100\ [\%] \quad (2)$$

where $S_{PC}$ is the maximum skin stress level occurring after the primary closure and $S_{NP}$ is the maximum stress after applying the suNPWT sys-

**Table 4**
Lateral displacement of the 'stiffness' variant models of a circular dressing along the shortest straight line between the internal material interface point in each dressing and the center point of the incision line, towards the incision line.

| Dressing | Lateral displacement [mm] |
|---|---|
| 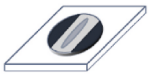 | 1.57 |
|  | 1.95 |
| 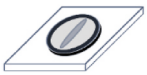 | 3.35 |
|  | 4 |
| 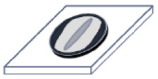 | 1.49 |
|  | 1.97 |
| 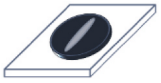 | 0.78 |
| 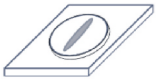 | 1.93 |
|  | 1.87 |

tem. In addition, morphological indices, including circularity, roundness, and circularity corrected by aspect ratio (noted '*R*' in Fig. 3a) were calculated for each dressing shape (Table 2, Fig. 3a) to investigate potential trends or correlations between the dressing shape and the extent of reduction in lateral peri-wound skin stresses ΔS (Equation (2)).

The 'shape' variants (Table 2, Fig. 3a) were chosen to span practical differences in roundness and symmetry while maintaining continuous peri-incisional coverage, guided by the influence zone framework [17–19]. Under this framework, the extent and intensity of peri-wound mechanostimulation depend on the delivered pressure and on the dressing characteristics, including size, shape, and material properties. Effective peri-wound coverage enlarges the stimulated tissue region. Accordingly, the focus was on relatively simple, manufacturable outlines that preserve continuity around the incision and are likely to be lower-cost than complex contours, while still allowing to isolate shape-driven effects on the influence zone.

***'Stiffness' model variants***: In a second step, after identifying the best performing dressing shape, i.e., the 'shape' model variant resulting in the greatest Δ*S* (Fig. 3a), additional focused analyses of this shape were further conducted. These additional analyses investigated whether further improvement in Δ*S* is possible using material stiffness variations in the best performing dressing shape, and whether regional variations in dressing stiffness can assist the incision-closure process under suNPWT. Specifically, to examine the influence of stiffness distribution within the superiorly-performing dressing shape, which was circular, eight different stiffness configurations were applied, namely, with: (a) stiffer lateral 'wings' having maximal width of 3.5 cm with respect to the core foam, (b) softer such 'wings', (c) stiffer symmetric circumferential ring having constant width of 1.9 cm with respect to the core foam, (d) softer such ring, (e) stiffer axisymmetric circumferential ring having a minimal width of 1.4 cm and maximal width of 3.5 cm with respect to the core foam, (f) softer such ring, (g) stiffer homogenous circular dressing, (h) softer homogenous circular dressing. The latter two, homogenous configurations were meant to generate benchmark data for the inhomogeneous 'stiffness' model variants. The volumes of each pair of lateral wings and each symmetric ring were set to be equal (157.5

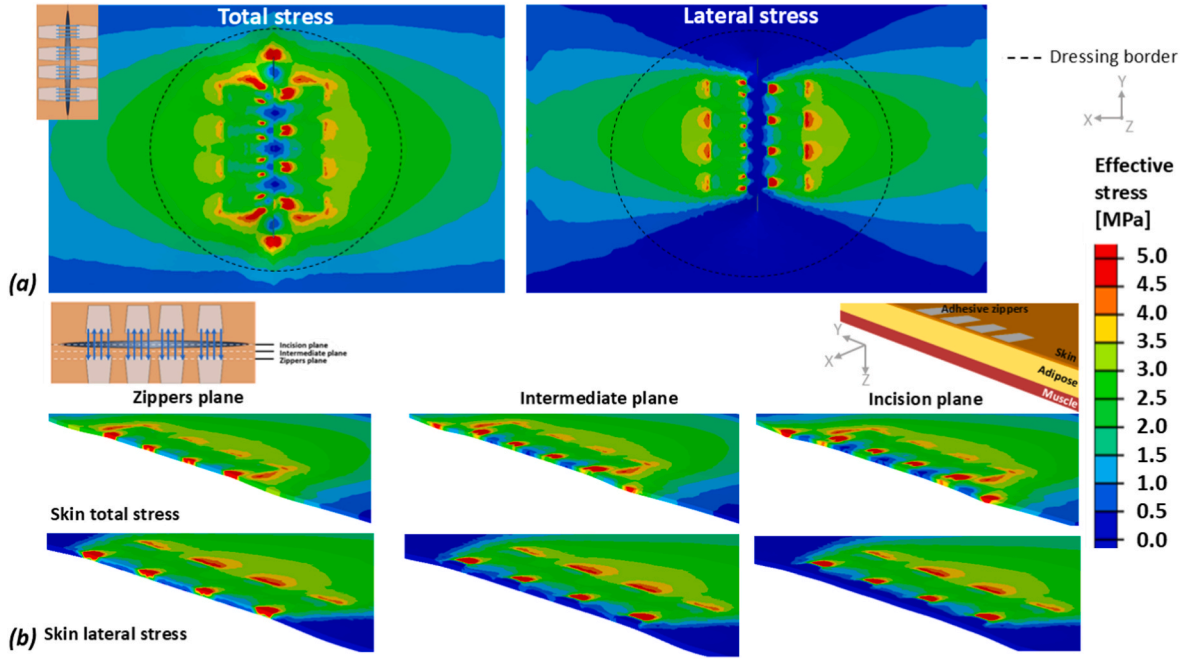


**Fig. 2.** Stress distributions in the peri-wound under a homogenous circular dressing: (a) Superior view of the effective stresses ("total stress" in the left frame) and of the lateral component of the stresses acting to close the incision ("lateral stress" in the right frame), showing stress concentrations around the zippers. (b) Cross-sectional views of subdermal stresses developed at the zippers plane (left frames), incision plane (right frames), and an intermediate plane (center frames), under a steady negative pressure of −125 mmHg (the zippers and dressing were hidden for clarity).

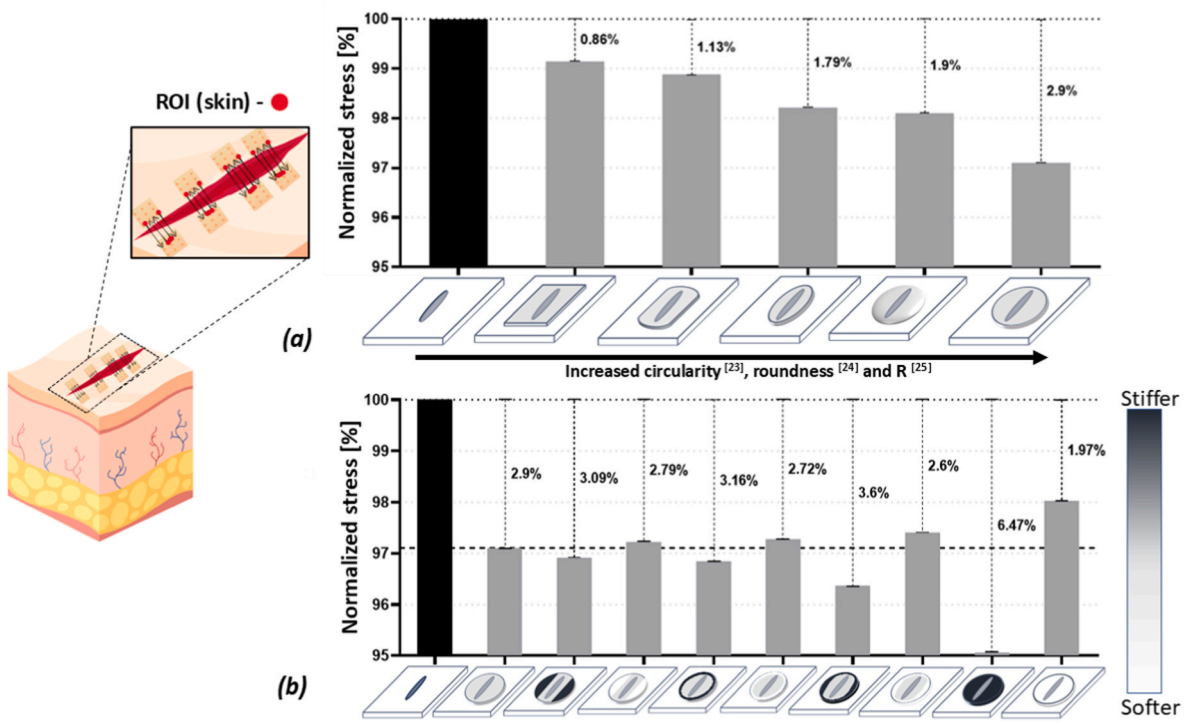


**Fig. 3.** Reduction in the lateral stress concentrations around the zippers (caused by the closure forces applied by the zippers during the primary closure), due to the participation effect of the negative pressure wound therapy in the closure of the incision, for the different dressing types that were tested in the current modelling: (a) The effect of transforming from a rectangular to a circular geometry for homogenous dressings, based on shape indexes of circularity, roundness and circularity corrected by aspect ratio ($R$), for which the numerical values per each dressing shape are provided in Table 3. (b) The effect of incorporation of stiffer or softer material regions in symmetric and axisymmetric designs of inhomogeneous dressings, and the effect of stiffer and softer materials in homogeneous dressings.

$cm^3$); the volume of the axisymmetric rings was mildly greater (198.3 $cm^3$). The mechanical properties of the "stiffer" and "softer" components of these 'stiffness' model variants are specified in Table 3. The aforementioned eight 'stiffness' model variants were constructed and analyzed to obtain their $\Delta S$ data, similarly to the 'shape' variants (Fig. 3b).

In addition, the lateral displacement of the dressing along the shortest straight line between the internal material interface point in each dressing and the center point of the incision line, towards the incision line, was calculated, per each 'stiffness' model variant. This measure evaluates how the regional stiffness differences influence the contribution of the dressing distortion under suNPWT to the closure work. For the benchmark homogenous dressings, where no material interface exists, the mean location of material interfaces for the other dressings was used as the reference point for the lateral displacement calculations. Both the lateral displacement and the $\Delta S$ data were normalized to their respective ranges, for the purpose of producing a scatter plot investigating their correlation.

### 2.6. Sensitivity analysis

A focused sensitivity analysis was conducted on four 'stiffness' model variants, the two best dressing design performers and two bounding cases (see Results and Fig. 4). For each model variant, five perturbations that reflected clinically plausible variability and design tolerances were made, as follows: (i) skin stiffness increased by 25 %, (ii) skin stiffness decreased by 25 %, (iii) incision length shortened by 20 %, (iv) dressing stiffness increased by 25 %, and, (v) dressing stiffness decreased by 25 %. Skin stiffness was chosen as skin stress concentrations are within the direct focus of this work, and for the same reason, varying the length of the incision was selected given that longer incisions require greater pulling forces for primary closure. The dressing stiffness determines the stiffness gradient with the skin and was therefore selected as an additional key parameter to include. The influence of variations in these three parameters (skin stiffness, incision length and dressing stiffness) was evaluated on the same outcome measures defined above, that is, reduction in the peak lateral skin stress ($\Delta S$, Equation (2)) and the lateral displacement towards the incision line (as a proxy for the closure work). The results of this sensitivity analysis were summarized in Table 5.

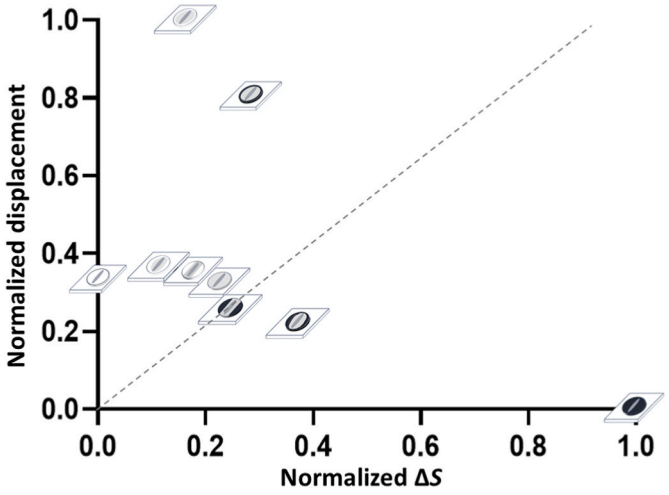


**Fig. 4.** A scatter plot of the normalized lateral stress reduction in skin near the zippers ($\Delta S$) versus the normalized lateral displacement at the internal material interface of each circular dressing. The dashed line represents equality between these two variables, i.e., a balance between reducing skin stress concentrations and promoting closure of the incision by means of the dressing. Absolute, non-normalized effective stress reductions ($\Delta S$) corresponding to the normalized percentages shown here are provided in Table A.1 (Appendix A).

To summarize, in total, thirty-three model variants were developed and analyzed (five focusing on dressing shape variants, additional eight on dressing stiffness variants for the preferred, circular shape and twenty for the sensitivity analysis). The $\Delta S$ data were calculated for all the model variants and lateral displacement data were further calculated for both the additional 'stiffness' model variants and the sensitivity analysis.

## 3. Results

We evaluated the influence of foam dressing shape and material stiffness configurations on peri-wound skin stress levels and extent of contribution to the lateral closure work of the incision following primary closure and application of suNPWT system.

### 3.1. Effect of the dressing shape

Among the five evaluated dressing shapes: rectangular, circular, elliptical, stadium and dome, the circular dressing demonstrated the greatest reduction in peak lateral stresses in the peri-wound skin ($\Delta S$ = 2.9 %; Fig. 3a). The dome-shaped dressing followed ($\Delta S$ = 1.9 %), while the conventional rectangular dressing yielded the lowest reduction in peri-wound skin stresses ($\Delta S$ = ~0.9 %). A positive correlation was observed between all the morphological indices of dressing shape (including circularity, roundness, and the corrected circularity index), and the $\Delta S$ values (Table 2), indicating that more circular suNPWT dressing designs have greater effectiveness at alleviating localized peri-wound skin stresses (Fig. 3a).

### 3.2. Effect of the material stiffness inhomogeneity and configuration

To determine whether spatial variations in material stiffness could further improve the stress-relieving performance of a circular dressing, eight additional configurations were analyzed: two with modified lateral "wings" (either stiffer or softer), two with circumferential symmetric rings (either stiffer or softer), two with circumferential axisymmetric rings (either stiffer or softer), and two homogenous dressings (either stiffer or softer), as shown in Fig. 3b.

Compared to the baseline uniform-stiffness circular dressing ($\Delta S$ = 2.9 %), the softer-wing, softer-symmetric ring, softer-axisymmetric ring and softer-homogenous dressing variants all showed slight reductions in skin stress alleviation performance ($\Delta S$ = 2.8 %, 2.7 %, 2.6 % and 2 %, respectively; values rounded to the first digit after the decimal point). In contrast, dressings incorporating stiffer regions around a soft core outperformed the uniform dressing baseline. Specifically, the dressing with the stiffer lateral wings yielded $\Delta S$ = 3.1 %, and the dressings with the stiffer-symmetric ring and the stiffer-axisymmetric ring yielded $\Delta S$ = 3.2 % and $\Delta S$ = 3.6 %, respectively. The stiffer-homogenous dressing variant yielded $\Delta S$ = 6.5 %, which alleviated skin stresses well, but at the price of nearly zero contribution to the lateral closure work through lateral displacement (Fig. 4).

To determine whether spatial variations in material stiffness could assist in the lateral closure process while still lowering the skin stress exposure, the lateral displacement was calculated for the additional 'stiffness' model variants (Table 4). The dashed line in the scatter plot of lateral displacement versus $\Delta S$ represents (theoretical) equality between these two variables, i.e., a balance between reducing skin stress concentrations and promoting closure of the incision by means of the suNPWT system and dressing. As could be expected, the homogenous circular soft dressing maximizes the lateral displacement but with poor contribution to the skin stress alleviation, which is opposite to the behavior of the homogenous stiff dressing. The circular dressing with a stiffer symmetric ring achieved the optimal performance of skin stress alleviation and contribution to the lateral closure work, while the dressing with a stiffer axisymmetric ring achieved the next best optimal performance for both parameters (Fig. 4). The dressing with the stiffer axisymmetric wings showed the best-balanced performance relative to

**Table 5**
Sensitivity of the outcome measures, i.e., reduction in peak lateral skin stress ($\Delta S$) and lateral displacement towards the incision line (as a proxy for the closure work), to changes in key model parameters.

| Parameter | Variation | Effects $\Delta S$ [%] | Lateral displacement [mm] | | | | | |
|---|---|---|---|---|---|---|---|---|
| | |  |  | 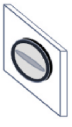 |  |  |  |  |
| Skin stiffness | Reference (no variation) | 3.6 | 3.16 | 6.47 | 1.97 | 1.49 | 3.35 | 0.78 | 1.93 |
| | −25 % | 5.21 | 4.73 | 9.32 | 2.91 | 1.5 | 3.36 | 0.79 | 1.93 |
| | +25 % | 2.49 | 2.15 | 4.56 | 1.42 | 1.49 | 3.34 | 0.78 | 1.93 |
| Dressing stiffness | −25 % | 2.6 | 2.39 | 4.8 | 1.49 | 1.68 | 3.4 | 0.74 | 1.95 |
| | +25 % | 4.49 | 3.96 | 8.05 | 2.38 | 1.34 | 3.24 | 0.77 | 1.93 |
| Incision length | −20 % | 1.89 | 1.83 | 3.05 | 1.41 | 1.51 | 3.36 | 0.8 | 1.96 |

the axisymmetric stiffer-ring dressing (Fig. 4).

### 3.3. Sensitivity analysis

The results of the sensitivity analysis on the chosen four model variants, namely, the two best dressing design performers: stiffer axisymmetric ring and stiffer symmetric ring; and two bounding cases: homogeneously stiff and homogeneously soft circular dressings (Fig. 4) are detailed in Table 5. Across all the five perturbations applied to each of these four circular dressing designs, the quantitative ranking was unchanged for both the $\Delta S$ and lateral displacement outcomes. Specifically, for the $\Delta S$ outcome measure, the consistent order was homogeneously stiff > stiffer axisymmetric ring > stiffer symmetric ring > homogeneously soft dressing. For the lateral displacement outcome measure, the order was: stiffer symmetric ring > homogeneously soft > stiffer axisymmetric ring > homogeneously stiff dressing. Taken together, these findings indicate that the comparative performance of the investigated dressing designs is not sensitive to moderate skin or dressing material stiffness changes within the tested range, nor to mild variation in the length of the surgical incision (Table 5).

## 4. Discussion

This study challenges a foundational yet underexamined assumption in suNPWT: The universal application of rectangularly shaped foam dressings, particularly for application on surgical incisions. Despite their widespread clinical use, rectangular dressings offer no biomechanical justification when examined through the lens of incision-support mechanobiology, and in particular in the aspect of improving the stress state of the peri-wound skin. In fact, our current *in silico* findings indicate that this longstanding design assumption appears biomechanically suboptimal and may limit the therapeutic potential of suNPWT. Specifically, we demonstrate that circular dressings markedly outperform rectangular designs in reducing peri-wound skin stresses, by more than a 3-fold factor ($\Delta S = 2.9$ % versus ~0.9 %). In other words, circular suNPWT dressings promote a more effective mechanical synergy with incision closure mechanisms (Fig. 3a). This is not simply a matter of aesthetics or geometric preference; it reflects a core biomechanical principle: Symmetry and geometry matter. Circular dressing designs eliminate corners or small radii of curvature, promoting smoother mechanical transitions to the peri-wound skin, which facilitate a more uniform redistribution of forces across the dressing-skin interface [25]. Conversely, rectangular dressings with their geometric discontinuities disrupt an effective lateral spread of the suNPWT-induced mechanical loads in the peri-wound, even when made of a softer material than skin, resulting in less effective incisional wound edge approximation and less effective reduction of the skin stresses associated with the primary closure. These disruptions may also lead to localized mechanical under-stimulation of the peri-wound skin at specific regions, particularly near the dressing corners and edges, due to poor force transmission across the curved sites and stiffness gradients. As a result, the area of effective tissue stimulation, the influence zone, is reduced [17–19]. This limits the ability of the dressing to support wound-edge approximation and mechano-activation of repair-relevant cells [19].

In contrast, a circular dressing effectively delivers radial force distributions, thereby promoting a more extensive influence zone, farther and deeper into the peri-wound. Specifically, the more symmetrical and round a dressing shape is, the better it can lower tissue stress concentrations under the isotropic external forces of negative pressure. This results in more uniform lateral tissue deformations, which in turn, increase both the influence zone and the ability of the applied dressing to assist in the primary wound closure, thereby participating more in the lateral forces of the primary closure, and ultimately, alleviating the stress concentrations on the skin regions subjected to the primary closure. Although conformability was not studied in this work, circular dressings may potentially conform more naturally to the body contours, providing continuous radial force distributions that better align with the architecture of cellular mechano-transduction zones. Lastly, when it comes to surgical incision treatments, a circular dressing covers more area perpendicular to the incision line with respect to a rectangular dressing having the same surface area, which implies that a circular dressing stimulates more of the peri-wound to induce cell migration towards the wound for repair [17].

To corroborate the current computational outputs with experimental evidence, we interpret the current $\Delta S$ data within a stress-dose framework, in the context of a pre-clinical porcine closed-incision study that combined bench measurements, FE analyses, and in vivo outcomes under suNPWT [4]. In the aforementioned study, consistent delivery of the intended negative pressure reduced the lateral tension along the incision and lowered the peri-suture skin stress concentrations over the therapy period, which were associated with earlier epidermal fusion and mildly superior biomechanical properties of the repaired skin [4]. Accordingly, we consider the peri-suture stress concentrations together with the cumulative exposure to these stress concentrations over time, as the physiologically and clinically meaningful information. In other words, we map our $\Delta S$ model outputs based on this theory, by relating the instantaneous $\Delta S$ to the time-integral of the stress, i.e., the stress-dose, for a given treatment window. This linkage provides important context for interpreting both the magnitude and the temporal persistence of the modelled stress reductions, and justifies the use of $\Delta S$ as a primary outcome in the present analysis. For example, if the stress reduction $\Delta S$ is approximately 2 %, which is the contribution of changing from a rectangular to a circular dressing shape (Fig. 3a), and this reduction remains roughly stable for only 24 h of suNPWT application (out of the several days of the typical suNPWT treatment period), the associated stress-dose difference will be approximately 48 % × h (i.e., the product of $\Delta S = 2$ % and time = 24 h). This illustrates how apparently small and potentially temporary stress differences can accumulate over time, and yield a fundamentally different mechanobiological environment for the peri-wound throughout the therapy period, and thus, ultimately, influence the wound healing outcomes. Accordingly, the integrative effect over the therapy time period, $\int \Delta S dt$ is the clinically oriented and relevant quantity, as opposed to single $\Delta S$ timepoint values (which are the data captured by the FE modeling). Indeed, the relevant porcine model study of surgical wound healing [4] links similar extents of "small" stress reduction and lateral closure work by a suNPWT system over the course of treatment to better biomechanical quality of the repaired skin, thereby supporting the clinical relevance of such "small" tissue stress exposure reductions in view of the nature of a dose-based suNPWT therapy.

This critique extends further when material stiffness of the dressing is considered. Our second set of simulations reported in this study examined regional stiffness variations within circular dressings. Here, designs featuring stiffer circumferential rings around a soft core, and particularly, the dressing with the perfectly symmetric stiffer ring, achieved the highest combination of stress relief and incision closure. Specifically, the dressing with the symmetric stiffer ring had $\Delta S = -3.2$ % (i.e., third-best stress relief performance) and lateral displacement of 3.35 mm (second-best support of closure work), which, considered together, is optimal (values were rounded to the first digit after the decimal point; Fig. 3b and Table 4). Importantly, these findings address another unchallenged convention in the wound care industry: The typical reliance on homogenous dressing materials in suNPWT. While stiffer homogenous dressings offered a relatively high skin stress relief ($\Delta S = 6.5$ %), they contributed minimally to the lateral closure work through a preferred direction of lateral displacement (0.78 mm), which is a key biomechanical action supporting incision approximation. On the other hand, a soft homogenous dressing, though highly deformable, lacks the directional control needed to meaningfully assist the closure work through a preferred material alignment, and accordingly, had a median lateral displacement for the range of dressings (Fig. 4 and Table 4). The current deficiency in meaningful directional displacements of homogeneous

dressings applied on incision wounds highlights the need for strategic material stiffness tuning to achieve coordinated dressing deformation patterns that support wound edge approximation in the treatment of surgical wounds.

Such coordination in the state of force delivery by suNPWT systems is not trivial to achieve. As Orlov & Gefen [18] emphasized, consistent and directed pressure application is essential to avoid uneven tissue loading, which can impede healing or even induce damage in surrounding tissues. While the dressing material stiffness is important, a uniform material design is not optimized to provide this consistency in practice [16]. Only regionally tuned dressings, specifically engineered to redirect pressure inward while stabilizing their periphery and pulling the edges of the incision wound together, can create the mechanical precision necessary for both protecting and repairing tissues. Furthermore, the continued adherence of the wound care industry to rectangular designs likely reflects a mindset rooted in manufacturing convenience, not in wound healing science or expected clinical performance. From a production standpoint, ring-core designs are neither exotic nor impractical. On the contrary, they require fewer unique components than the wing-based variants studied here, and can be fabricated through the well-established lamination or molding techniques. While implementation of circular dressings having a stiffer ring at the periphery and softer core may require retooling or regulatory reevaluation, the biomechanical and clinical benefits justify such investment.

This is the first study to demonstrate that it is not only the stiffness of the suNPWT dressing, but also its spatial distribution, when paired with an optimized shape, that significantly impacts biomechanical support for incision closure. Limitations that should be mentioned include the use of a certain negative pressure therapy level (−125 mmHg), which, while accepted in the field, can substantially deviate from pressure levels used in some commercial devices by different manufacturers. In addition, we enforced tied contact at the skin-adhesive, skin-dressing, and adhesive-dressing interfaces, which is a simplifying assumption that does not capture possible interfacial slip arising from fascial sliding or imperfect adhesion. This choice was made to ensure numerical tractability and to isolate the effects of dressing shape and stiffness on the reported outcomes. We acknowledge that allowing frictional or cohesive-sliding contact could influence local stress transfer and displacement fields, and we identify incorporation of calibrated frictional parameters and peel mechanics as a priority for future work. We also did not consider fragile skin and tissue conditions, surgical complications affecting the tissue biomechanical behavior and properties, excess or persistent edema and other pathophysiological changes affecting skin or subdermal tissue stiffness. Nonetheless, the trends revealed here are robust across geometries and dressing materials, and they raise fundamental questions that industry stakeholders can no longer afford to ignore.

To conclude, the rectangular suNPWT dressing warrants critical reevaluation. Our current *in silico* work demonstrates that a rectangular dressing for suNPWT is incompatible with the influence zone principle, fails to harness the full potential of mechanostimulation, and underperforms in both skin stress concentration mitigation and incision closure support. This work suggests that circular dressings with engineered stiffness gradients may offer a scientifically and clinically superior alternative to the traditional rectangular shapes. These findings support a shift in dressing design considerations, guided by emerging insights from *in silico* bioengineering and mechanobiology science. Future work should further validate these *in silico* insights through clinical research comparing healing rates, quality of the repaired tissues, and complication incidence across dressing shapes and stiffness profiles. In addition, broader exploration of the joint shape-material design space using surrogate modeling methods such as Kriging is feasible. Future studies could also model interfacial mechanics more realistically, by incorporating friction and sliding at the skin-dressing and skin-adhesive interfaces, including peel and cohesive behavior, to assess their impact on local stress transfer and closure assistance. Such future *in silico* and clinical validation work could further support 'stepping out of the box' of rectangular dressings and creating an evidence-based industry and regulatory shift in NPWT dressing design.

## Conflict of interest statement

The authors declare that they have no conflict of interest.

## Acknowledgements

This work was partially supported by the Israeli Ministry of Innovation, Science and Technology: Breakthrough Research Program Grant no. 1001702603, awarded to Professor Amit Gefen in 2023.

## APPENDIX A

**TABLE A.1**
Absolute (non-normalized) reductions in peak lateral skin stress used for the $\Delta S$ percentage calculations reported in the body of the text and depicted in Figs. 3 and 4.

| Dressing | Absolute stress reduction [MPa] |
|---|---|
| 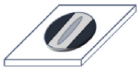 | 0.62 |
|  | 0.56 |
| 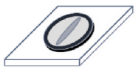 | 0.63 |

(*continued on next page*)

**TABLE A.1** (*continued*)

| Dressing | Absolute stress reduction [MPa] |
|---|---|
|  | 0.54 |
| 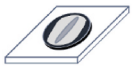 | 0.72 |
|  | 0.52 |
|  | 1.29 |
|  | 0.39 |
|  | 0.58 |

## References


[1] Bobkiewicz A, Banasiewicz T, Ledwosinski W, Drews M. Medical terminology associated with Negative Pressure Wound Therapy (NPWT). Understanding and misunderstanding in the field of NPWT. Negat Press Wound Ther 2014;1:69–73.

[2] Saxena V, Hwang CW, Huang S, Eichbaum Q, Ingber D, Orgill DP. Vacuum-assisted closure: microdeformations of wounds and cell proliferation. Plast Reconstr Surg 2004 Oct;114(5):1086–96. https://doi.org/10.1097/01.prs.0000135330.51408.97. discussion 1097-8 PMID: 15457017.

[3] Argenta LC, Morykwas MJ. Vacuum-assisted closure: a new method for wound control and treatment: clinical experience. Ann Plast Surg 1997 Jun;38(6):563–76. ; discussion 577. PMID: 9188971.

[4] Orlov A, Gefen A. The potential of a canister-based single-use negative-pressure wound therapy system delivering a greater and continuous absolute pressure level to facilitate better surgical wound care. Int Wound J 2022 Oct;19(6):1471–93. https://doi.org/10.1111/iwj.13744. Epub 2022 Jan 20. PMID: 35048527; PMCID: PMC9493241.

[5] Katzengold R, Topaz M, Gefen A. Tissue loads applied by a novel medical device for closing large wounds. J Tissue Viability 2016 Feb;25(1):32–40. https://doi.org/10.1016/j.jtv.2015.12.003. Epub 2015 Dec 21. PMID: 26750452.

[6] Ritchie SA. Skin surgery: prevention and treatment of complications. Retrieved from UpToDate; 2018. Available from: https://www.uptodate.com/contents/skin-surgery-prevention-and-treatment-of-complications.

[7] Commander SJ, Chamata E, Cox J, Dickey RM, Lee EI. Update on postsurgical scar management. Semin Plast Surg 2016 Aug;30(3):122–8. https://doi.org/10.1055/s-0036-1584824. PMID: 27478420; PMCID: PMC4961501.

[8] Markets and Markets Research Pvt Ltd. Solventum (US) and Smith+Nephew (UK) are leading players in the negative pressure wound therapy market. Pune; 2025. IN Available from: https://www.marketsandmarkets.com/ResearchInsight/negative-pressure-wound-therapy-market.asp.

[9] Adie GC, Collinson SJ, Fryer CJ, Hartwell EY, Nicolini D, Peron YL, inventors Smith, Nephew PLC, assignee. Wound dressing and method of use. United States patent US 2015;9. Available from: https://patentimages.storage.googleapis.com/06/f3/2c/d97dbade8cda90/US9061095.pdf.

[10] National Institute for Health and Care Excellence (NICE). Medical technology scope: PICO single-use negative pressure wound therapy system for closed surgical incisions. London: NICE; 2018 Aug. Available from: https://www.nice.org.uk/guidance/mtg43/documents/final-scope-2.

[11] Schwartz D, Gefen A. The biomechanical protective effects of a treatment dressing on the soft tissues surrounding a non-offloaded sacral pressure ulcer. Int Wound J 2019 Jun;16(3):684–95. https://doi.org/10.1111/iwj.13082. Epub 2019 Jan 29. PMID: 30697945; PMCID: PMC7949468.

[12] Wu Z. A method for eliminating the effect of 3-D bi-material interface corner geometries on stress singularity. Eng Fract Mech 2006;73(7):953–62. Available from: https://www.sciencedirect.com/science/article/pii/S0013794405002754?via%3Dihub.

[13] Wilkes RP, Kilpad DV, Zhao Y, Kazala R, McNulty A. Closed incision management with negative pressure wound therapy (CIM): biomechanics. Surg Innov 2012;19:67–75. https://doi.org/10.1177/1553350611414920.

[14] Sussman G. Technology and product reviews. Wound Repair Regen 2006;14(6):647–8.

[15] Wilkes R, Zhao Y, Kieswetter K, Haridas B. Effects of dressing type on 3D tissue microdeformations during negative pressure wound therapy: a computational study. J Biomech Eng 2009;131(3):031012. https://doi.org/10.1115/1.2947358.

[16] Orlov A, Gefen A. How influential is the stiffness of the foam dressing on soft tissue loads in negative pressure wound therapy? Med Eng Phys 2021 Mar;89:33–41. https://doi.org/10.1016/j.medengphy.2021.02.001. Epub 2021 Feb 3. PMID: 33608123.

[17] Gefen A. The influence zone: a critical performance measure for negative pressure wound therapy systems. Br J Nurs 2022 Aug 11;31(15):S8–12. https://doi.org/10.12968/bjon.2022.31.15.S8. PMID: 35980923.

[18] Orlov A, Gefen A. Effective negative pressure wound therapy for open wounds: the importance of consistent pressure delivery. Int Wound J 2023 Feb;20(2):328–44. https://doi.org/10.1111/iwj.13879. Epub 2022 Jul 11. PMID: 35818745; PMCID: PMC9885467.

[19] Gefen A, Russo S, Ciliberti M. Revisiting negative pressure wound therapy from a mechanobiological perspective supported by clinical and pathological data. Int Wound J 2024 Dec;21(12):e70098. https://doi.org/10.1111/iwj.70098. PMID: 39694469; PMCID: PMC11655127.

[20] Katzengold R, Topaz M, Gefen A. Dynamic computational simulations for evaluating tissue loads applied by regulated negative pressure-assisted wound therapy (RNPT) system for treating large wounds. J Tissue Viability 2018 May;27(2):101–13. https://doi.org/10.1016/j.jtv.2017.10.004. Epub 2017 Oct 28. PMID: 29100715.

[21] Palevski A, Glaich I, Portnoy S, Linder-Ganz E, Gefen A. Stress relaxation of porcine gluteus muscle subjected to sudden transverse deformation as related to pressure sore modeling. J Biomech Eng 2006 Oct;128(5):782–7. https://doi.org/10.1115/1.2264395. PMID: 16995767.

[22] INEOS Olefins & Polymers USA. A60-70-162 polyethylene homopolymer: technical data sheet. Houston, TX: INEOS; 2014. Available from: https://www.ineos.com/show-document/?grade=A60-70-162&bu=INEOS%20O%20%26%20P%20USA&documentType=Technical%20Data%20Sheet&docLanguage=US-EN&version=54c6629317b569a3f13ae3c8aabbb1f5.

[23] Takashimizu Y, Iiyoshi M. New parameter of roundness R: circularity corrected by aspect ratio. Prog Earth Planet Sci 2016;3:2.

[24] Ritter N, Cooper J. New resolution independent measures of circularity. J Math Imag Vis 2009;35:117–27. https://doi.org/10.1007/s10851-009-0158-x.

[25] Gefen A. The selection of cushioning and padding materials for effective prophylaxis of medical device-related pressure ulcers: clinical intuition does not always work. Wounds Int 2022;13(1):10–9.